Received: 28 November 2020 | Accepted: 10 September 2021

DOI: 10.1111/jvim.16270

STANDARD ARTICLE

Journal of Veterinary Internal Medicine Open Access

ACVIM American College of Veterinary Internal Medicine

Neuronal current imaging: An experimental method to investigate electrical currents in dogs with idiopathic epilepsy

Daniela M. Unger[1] | Roland Wiest[2] | Claus Kiefer[2] | Mathieu Raillard[3] | Guillaume F. Dutil[4] | Veronika M. Stein[4] | Daniela Schweizer[1]

[1]Division of Clinical Radiology, Department of Clinical Veterinary Medicine, Vetsuisse Faculty, University of Bern, Bern, Switzerland

[2]Support Center of Advanced Neuroimaging (SCAN), Institute of Diagnostic and Interventional Neuroradiology, Inselspital Bern, University of Bern, Bern, Switzerland

[3]Division of Clinical Anesthesiology, Department of Clinical Veterinary Medicine, Vetsuisse Faculty, University of Bern, Bern, Switzerland

[4]Division of Clinical Neurology, Department of Clinical Veterinary Medicine, Vetsuisse Faculty, University of Bern, Bern, Switzerland

Correspondence
Daniela Schweizer, Laenggassstr. 128, 3012 Bern, Switzerland.
Email: daniela.schweizer@vetsuisse.unibe.ch

Abstract

Background: The diagnosis of idiopathic epilepsy (IE) in dogs is based on exclusion of other potential causes of seizures. Recently, a novel magnetic resonance imaging (MRI) sequence that utilizes a variant of the rotary saturation approach has been suggested to detect weak transient magnetic field oscillations generated by neuronal currents in humans with epilepsy.

Hypothesis/Objectives: Effects on the magnetic field evoked by intrinsic epileptic activity can be detected by MRI in the canine brain. As proof-of-concept, the novel MRI sequence to detect neuronal currents was applied in dogs.

Animals: Twelve dogs with IE and 5 control dogs without a history of epileptic seizures were examined.

Methods: Prospective case-control study as proof-of-concept. All dogs underwent a clinical neurological examination, scalp electroencephalography, cerebrospinal fluid analysis, and MRI. The MRI examination included a spin-locking (SL) experiment applying a low-power on-resonance radiofrequency pulse in a predefined frequency domain in the range of oscillations generated by the epileptogenic tissue.

Results: In 11 of 12 dogs with IE, rotary saturation effects were detected by the MRI sequence. Four of 5 control dogs did not show rotary saturation effects. One control dog with a diagnosis of neuronal ceroid lipofuscinosis had SL-related effects, but did not have epileptic seizures clinically.

Conclusions and Clinical Importance: The proposed MRI method detected neuronal currents in dogs with epileptic seizures and represents a potential new line of research to investigate neuronal currents possibly related to IE in dogs.

KEYWORDS
dog, MRI, NCI, pcSIRS, seizure, veterinary

1 | INTRODUCTION

Epilepsy is a common neurological disorder in dogs with a prevalence of 0.6% to 0.75% in the general dog population.[1] The diagnosis of

Abbreviations: APL, adjustable pressure limiting; BOLD, blood oxygen level-dependent; CSF, cerebrospinal fluid; EEG, -; HFO, high-frequency oscillation; IE, idiopathic epilepsy; MRI, magnetic resonance imaging; NCI, neuronal current imaging; pcSIRS, phase-cycled stimulus-induced rotary saturation; PEEP, positive end expiratory pressure; SL, spin-locking; TA, time of acquisition; TCI, target-controlled infusion; TE, echo time; TR, repetition time.

idiopathic epilepsy (IE) in dogs is based on exclusion of other potential causes of seizures. Although in the majority of humans, structural inborn errors of brain maturation, insults during brain maturation, or acquired cerebral lesions are responsible for epileptic disorders, magnetic resonance imaging (MRI) has identified structural abnormalities only in 2.2% of dogs <6 years of age with seizures.[1-5] Unfortunately, less than one-third of seizuring dogs show abnormalities during short time scalp electroencephalography (EEG) recording.[6-9] These negative findings hamper appropriate syndromal classification, and the differentiation of movement disorders is sometimes challenging. Noninvasive additive techniques that remain sensitive even under general anesthesia therefore are necessary to overcome some of these challenges and to enable accurate diagnosis of IE.[10]

In recent years, efforts have been made to detect neuronal activity in the brain using MRI. One of the proposed methods to achieve MRI signals of neuronal activity (neuronal current imaging [NCI]) is to allow resonant interactions between the neuronal currents and spin magnetization.[11] A mechanism to allow these interactions is the spin lock mechanism, which was introduced in 1961 and uses a low frequency, so-called spin locking pulse, to lower the resonance frequency within the magnetic field. If transient neuronal currents at the same frequency as the spin-locking pulse are present, a resonant saturation effect occurs and the spins are locked in transverse magnetization.[12] The resonant saturation effect, also known as rotary saturation, can be measured and is higher in epilepsy compared to the normal brain, because amplitudes of the neuronal currents and current dipole strengths are significantly higher.[11] A novel variant of such a spin-locking rotary saturation sequence recently has been proposed that uses cycles of spin lock (SL ON) and non-spin lock (SL OFF) to decrease other, nonepilepsy related, effects.[13] Accordingly, the name of the sequences has been changed to phase-cycled stimulus-induced rotary saturation (pcSIRS) and the sequence is currently under development and being considered for patenting.[13] The pcSIRS was shown to visualize modulations of the local electromagnetic fields within the epileptic brain of humans. When the pcSIRS was applied in 8 human patients with focal epilepsy, focal clusters of rotary saturation effects were detected in all patients. In 2 patients who underwent surgical resection of the seizure onset zone, resulting in excellent seizure control after surgery, the rotary saturation effects were no longer detectable at follow-up MRI suggesting that the pcSIRS effect matched the seizure-onset zone.[13]

The aim of our prospective proof-of-concept study was to determine if a novel MRI sequence named pcSIRS could detect rotary saturation effects in dogs with IE examined under general anesthesia. We hypothesized that rotary saturation effects suggesting the presence of high frequency oscillations (HFOs) would be seen in dogs with IE but not in nonepileptic control dogs.

2 | MATERIALS AND METHODS

2.1 | Animals

This proof-of-concept study was performed as a prospective clinical diagnostic test evaluation and in agreement with local ethical regulations (Veterinary Office, Canton of Bern, Switzerland—BE15/18 and No. 29935). All dogs were client-owned dogs and all owners signed a written formal consent.

Twelve dogs with an ongoing history of clinically observable epileptic seizures were included (dogs with IE), regardless of whether treatment with antiseizure drugs had already been started or not. The age at first seizure was between 1 and 8 years of age. Inclusion criteria for dogs with IE were normal results of physical and interictal neurological examinations, CBC, and serum biochemistry. Age at seizure onset, number of observed seizure events since the first seizure (1-10, 10-50, >50 seizure events), seizure frequency, and time between the last seizure event and MRI were recorded.

In the control group, 5 dogs without a history of epileptic seizures were included. These dogs were clinically healthy or had undergone MRI of the brain for reasons other than clinically observed seizures.

2.2 | Anesthesia protocol

Food was withheld approximately 8 hours before the procedure but water was allowed ad libitum until 30 minutes before premedication. An IV catheter (Jelco 2 IV Catheter Radiopaque, Smiths Medical International Ltd, Ashford, UK) was placed in a cephalic vein. Premedication included butorphanol (Morphasol, 10 mg/mL, Dr E. Graeub AG, Berne, Switzerland) 0.3 mg/kg administered IV in all but 2 occurrences in which it was administered IM together with dexmedetomidine 10 μg/kg (Dexdomitor, 0.5 mg/mL, Provet AG, Lyssach, Switzerland) because dogs were noncooperative. Animals then were positioned in sternal recumbency on an MRI-compatible table and preoxygenated for 3 to 5 minutes using a loosely applied facemask with a fresh gas flow of 10 L/min through a circle breathing system connected to an anesthesia station (Fabius MRI anesthesia machine, Dräger, Lübeck, Germany) with the adjustable pressure limiting (APL) valve closed. Propofol (Propofol 1%, Fresenius Kabi, Oberdorf, Switzerland) target-controlled infusion (TCI) was used for induction of anesthesia throughout the EEG examination and during acquisition of the pcSIRS sequence using a syringe driver (Graseby 3400 Anesthesia Pump, Graseby Medical Ltd, Watford Herts, UK) connected to a computer equipped with TCI software (Computer Controlled Infusion Pump CCIP program version 2.4, Department of Anesthesia and Intensive Care, The Chinese University of Hong Kong, China) using previously published pharmacologic data.[14] A plasma propofol concentration of 3 to 5 ng/mL was targeted to ensure sufficient muscle relaxation and absence of gag reflex and cough during intubation. The trachea was intubated using single-use orotracheal tubes. The inspired fraction of oxygen was set to 40%, the APL valve was opened, and animals were connected to the circle breathing system. Cuffs were inflated using a 5-mL syringe until no leak was audible at an airway pressure of 20 cm H_2O. Controlled mechanical ventilation was initiated immediately after intubation using a volume-controlled mode with a tidal volume of 12 mL/kg and a positive end expiratory pressure (PEEP) of 5 cm H_2O. Maximum peak pressure was <20 cm H_2O. Initial respiratory rate was 15 breaths/min and then adjusted to maintain end tidal carbon dioxide between 30 and 35 mm Hg; the inspiratory time was set to

maintain an inspiratory-to-expiratory ratio of 1 : 2.5 and absence of development of auto-PEEP was ensured by observation of the flow-time spirometry loops. The plasma propofol concentration target was decreased to 2.5 to 3.5 ng/mL to maintain general anesthesia. After ensuring appropriate depth of anesthesia (absence of gag and palpebral reflexes, decreased jaw and muscular tone, and ventral rotation of the eye), atracurium 0.3 mg/kg (Atracurium Labatec, 10 mg/mL, Labatec Pharma SA, Geneva, Switzerland) was administered IV. In 3 dogs (dogs 1, 16, and 17), propofol was titrated to effect for induction and a continuous rate infusion of 0.15 to 0.4 mg/kg/min was used to maintain anesthesia.

Monitoring was clinical and by instrument using a multiparametric anesthesia monitor (Philips Invivo Expression MRI, Soma Technology, Inc, Bloomfield, Connecticut). Variables measured included peripheral hemoglobin saturation (SpO_2), capnography, spirometry, temperature, and noninvasive blood pressure (oscillometric technique) with a cuff positioned at the level of 1 of the dorsal metatarsal arteries (cuff width approximately 40% of the circumference of the limb). Plasmalyte solution (Baxter AG, Opfikon, Switzerland) was administered at 5 mL/kg/h during the first hour of general anesthesia, after which it was decreased by 25% per hour until a rate of 2 mL/kg/h was achieved.

To avoid prolonged recovery, propofol administration was stopped after the acquisition of the pcSIRS sequence and dexmedetomidine 1 to 2 μg/kg was administered IV. Anesthesia thereafter was maintained using sevoflurane (Sevorane, AbbVie AG, Baar, Switzerland; 2%-3% vaporizer setting) vaporized in the same oxygen-air mixture. Although mean duration of anesthesia was 130 ± 25 minutes, glycopyrrolate (10 μg/kg) and neostigmine (50 μg/kg; Robinul-Neostigmine, Glicopyrrolate Bromide, 5 mg/mL; Neostigmine methylsulfate 2.5 mg/mL, Sintetica S.A., Mendrisio, Switzerland) were injected IV at the end of the procedure. Sevoflurane administration then was discontinued, respiratory rate was decreased on the ventilator and dogs were allowed to breathe spontaneously. After extubation, oxygen was administered via facemask and dogs were closely monitored until they were able to stand.

2.3 | Electroencephalography

In all dogs, a scalp EEG was recorded 15 minutes immediately after induction of general anesthesia and before MRI (Lifelines Ltd Trackit MK3-EEG/Polygraphy Recorder, Stockbridge, UK) using 13 electrodes and 1 ground as well as 1 reference electrode. The electrodes were placed SC over the skull (Figure 1) according to previous descriptions using stainless steel needles (Natus neurology, 12 mm, 27 gauge, Middleton, Wisconsin).[15] The position of the electrodes was adapted to the shape of the skull and was slightly different between brachycephalic and meso- and dolicho-cephalic dog breeds.[16]

2.4 | Magnetic resonance imaging parameters (pcSIRS and structural imaging)

Magnetic resonance imaging of the brain was performed using a high-field MRI scanner (Siemens Magnetom Prisma^{fit} 3T, Siemens, Erlangen, Germany). Dogs were positioned in sternal recumbency with the head in a knee or head coil depending on the size of the head. The imaging protocol consisted of a 1 mm isotropic voxel 3-dimensional (3D) magnetization prepared rapid gradient echo (MPRAGE) sequence with Fat-Navigator echoes for retrospective motion correction.[17] The sequence parameters were as follows: time of acquisition (TA): 5 minutes, 27 seconds; voxel size: 1.0 × 1.0 × 1.0 mm; acquisition matrix and field of view were adapted according to size of the skull and varied between 230 to 256 (matrix) and 230to 256 mm; parallel imaging technique: generalized autocalibrating partial parallel acquisition; repetition time (TR) 2330.0 ms; echo time (TE) 3.03 ms; magnetization preparation: nonselective inversion recovery: time of inversion: 1100 ms; flip angle 8°; slices per slab 176; bandwidth 130 Hz/Px; 139 navigator echoes.

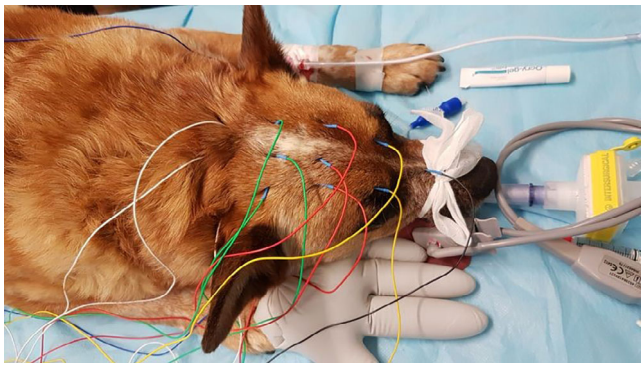

FIGURE 1 Placement of EEG-electrodes shown on the example of a control dog. EEG, electroencephalography

This sequence was followed by B0 mapping and pcSIRS with the following sequence parameters: TA: 6 minutes 17 seconds; voxel size: 3.6 × 3.6 × 4.0 mm; matrix: 64 × 64, field of view: 200, pixel size: 3.14 × 3.1 mm, slice thickness 4 mm; number of slices: 18; TR 139.55 ms; TE 29.12 ms; measurements: 150; base resolution 64; spin-lock pulse times 2 × 35 000 μs; bandwidth 1950 Hz/Px.

The acquisition was followed by morphological sequences to exclude structural changes: T2-weighted space 3D (slice thickness 0.9 mm; TE 408 ms, TR 3200 ms), 3D T2-weighted fluid attenuation inversion recovery (FLAIR; slice thickness 1 mm, TE 336 ms, TR 5000 ms, TI 1800 ms), T2-weighted turbo spin echo sequence in transverse plane (slice thickness 3 mm, TE 103 ms, TR 5070 ms). A post-contrast 3D MPRAGE sequence was acquired after administration of 0.15 mmol gadolinium/kg IV (Clariscan acidum gadotericum, 0.5 mmol gadolinium/mL, GE Healthcare AG, Opfikon, Switzerland).

2.5 | Postprocessing

For each voxel, the signal from SL OFF and SL ON (for each of the SL frequencies) was deconvolved pairwise for each measurement (n = 150) to obtain a corrected signal for the 150 measurements for quantification. Median filtering and contrast-limited adaptive histogram equalization were applied to minimize noise and to avoid amplifying any noise, respectively (Matlab R2014a). Main B0 field

distortion corrections were applied using previously proposed approach.[18] For coregistration of the NCI results with the structural 3D-T1 dataset, SPM8 software was used. In order to easily identify the gray and white matter contributions on the resulting NCI maps, the latter were masked with the segmented T1 maps using the SPM8 segmentation module and the difference maps (SL minus non-SL acquisition) were transformed to indicate the cluster with the maximum *z* score. Further information on the different postprocessing steps is available in the Supporting Information.

2.6 | Morphologic MRI analysis

For all dogs, the morphologic sequences (T2-weighted FLAIR, T2-weighted, and T1-weighted sequences pre- and post-contrast) were evaluated for structural abnormalities. In 1 dog with a subjective difference in hippocampal volume, a morphometric analysis was performed by manual segmentation with MRIcro (http://www.mricro.com). The transverse plane was defined as the default plane for labeling; volumetric definitions were consistently used by interfering with the cortical borders of the hippocampus in the sagittal and dorsal planes. Using anatomic landmarks, a 3D representation of the hippocampus was generated and volumes were extracted.[19,20] The asymmetry was calculated according to an asymmetry index = *(volume right hippocampus - volume left hippocampus) / (volume right hippocampus + volume left hippocampus)* × 100.

2.7 | Cerebrospinal fluid examination

After MRI examination, cerebrospinal fluid (CSF) samples were collected from the dogs with IE from the cerebellomedullary cistern using a spinal needle (BD Spinal Needle, 22 Gauge, Becton Dickinson S.A., Madrid, Spain). The CSF analysis was performed within 30 minutes after collection and considered as normal with cell count <5 cells/μL and protein concentration <0.25 g/L.

2.8 | Statistics

Accuracy of pcSIRS to discriminate between dogs with IE and control dogs without epileptic seizures was evaluated by determining the number of true positive, true negative, false positive, and false negative results.

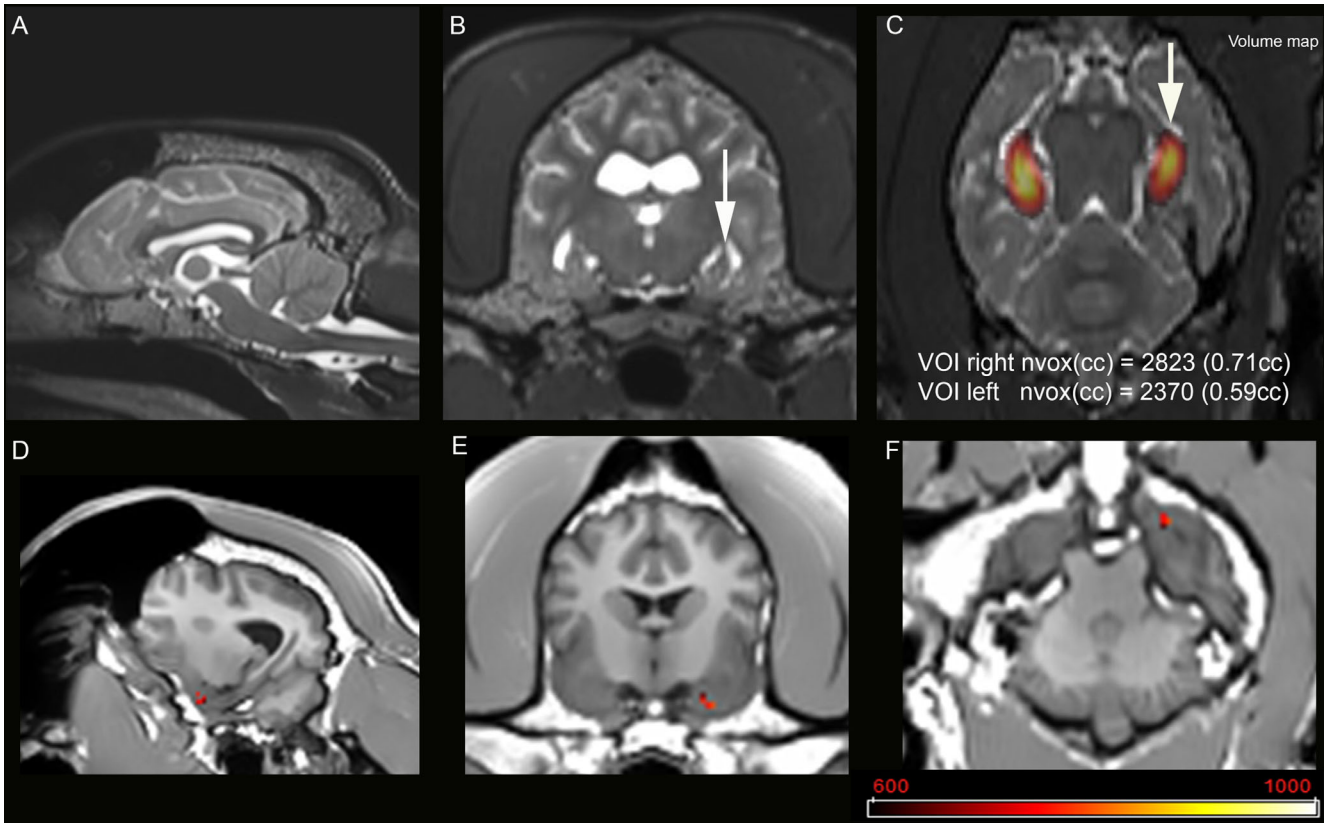

FIGURE 2 MR images of a 3-year-old male Small Bernese Dog with focal motor and focal behavioral seizures. Sagittal (A) and transverse (B) reconstruction of a T2-weighted space 3D sequence show no structural abnormality other than a mild volume loss of the left hippocampus (white arrow) that was confirmed on a volume map with lower voxel numbers of the left compared to the right hippocampus. The NCI maps are based on *z* scores using a rescaling factor to visualize subtle differences in a graphically sufficient manner (0-1000). On pcSIRS (D, E, F), a focal rotary saturation effect (red color) is visible within the left hippocampus. MR, magnetic resonance; NCI, neuronal current imaging; pcSIRS, phase-cycled stimulus-induced rotary saturation

3 | RESULTS

The mean age of dogs with IE was 4.1 years. Six dogs were male (4 intact, 2 neutered) and 6 were female (2 intact, 4 spayed). Seven of the 12 dogs showed epileptic seizures despite antiseizure treatment, the remaining 3 dogs had not yet received antiseizure medications. The signalment, time of seizure onset, number of seizure events, seizure frequency, and time between last seizure and MRI results of the dogs with IE are presented as Supporting Information.

In 1 dog (dog 9), a seizure event with loss of consciousness, muscle twitching on the head, and severe salivation occurred approximately 1 minute after sedation with butorphanol IV. Intravenous injection of a benzodiazepine stopped the seizure and allowed induction of general anesthesia.

Five dogs were included in the control group. The mean age was 5.2 years. Signalment, clinical history, and results of physical examination as well as MRI findings are presented as Supporting Information.

Scalp EEG was performed in all dogs, but evaluation was limited in dog 1 for technical reasons. The EEGs showed relatively slow frequency (mainly theta and delta activity) and low amplitudes compatible with basic rhythm in anesthetized dogs with IE as well as in all control dogs. Interictal epileptic discharges were not detected in any of the EEGs.

Magnetic resonance imaging of the brain identified no structural abnormalities in the dogs with IE except for mild hippocampal asymmetry in 1 dog (dog 1, Figure 2). Volumetry of the hippocampus indicated volume loss of the left hippocampus in comparison to the right with the left hippocampus encompassing 2370 voxels (0.59 cm^3) compared to 2823 voxels for the right hippocampus (0.71 cm^3). The asymmetry index was 9.2 indicating a strong asymmetry and volume loss with respect to the left-sided hippocampus.[19,20]

In the control group, 1 dog (dog 13) had moderate hydrocephalus and a left-sided neuropathy of cranial nerves VII and VIII. Dog 14 had mild signs of brain atrophy. Otherwise, no structural brain abnormalities were detected in the control dogs.

The pcSIRS yielded a positive result in 11 of 12 dogs with IE (Figures 2 and 3 as examples of rotary saturation effects within the brain). Of these 11 dogs, none yielded a positive result for the SL

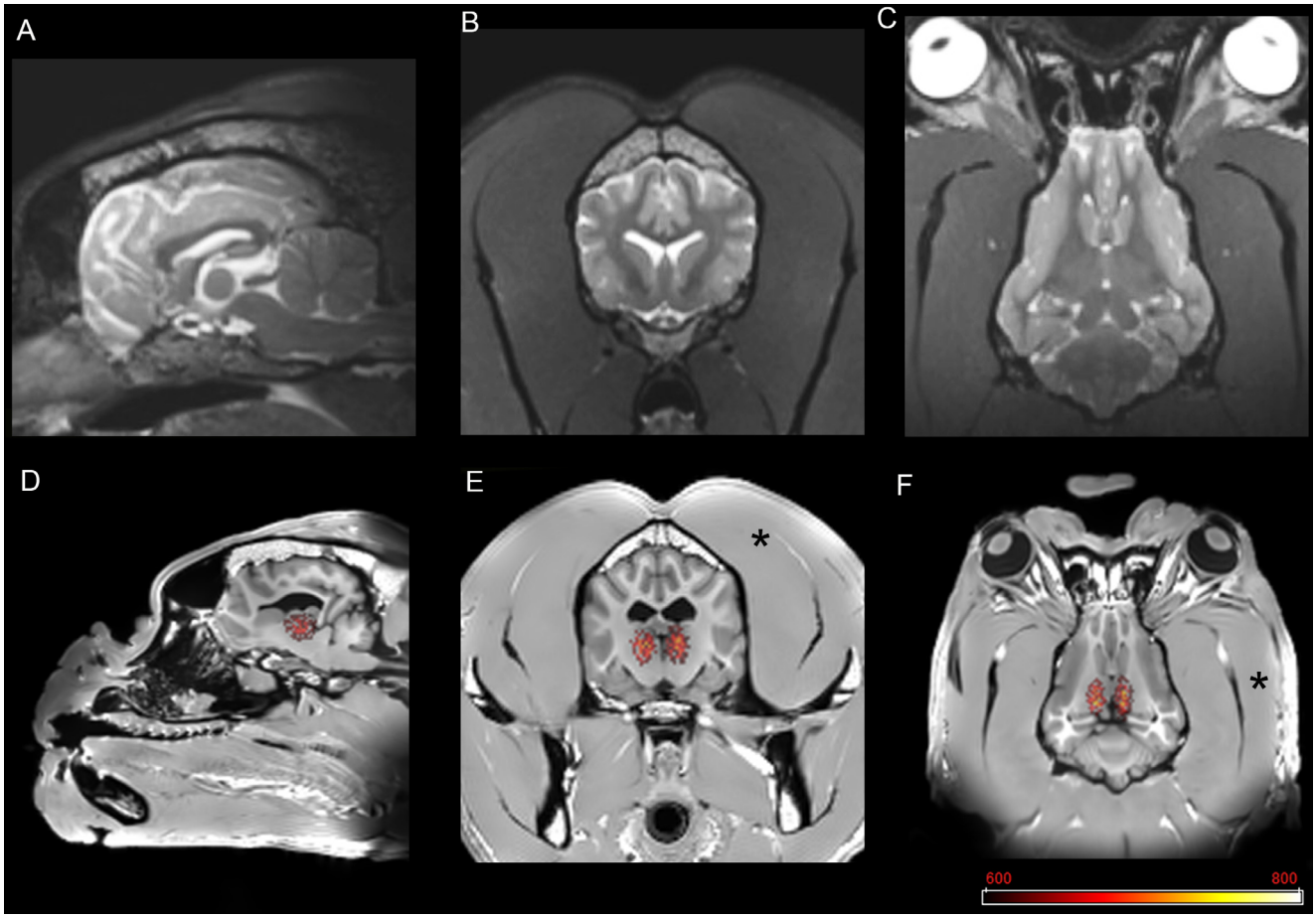

FIGURE 3 MRI images of a 5-year-old female Old English Bulldog with generalized tonic clonic seizures. No abnormalities were noted on sagittal (A), transverse (B), and dorsal (C) reconstructions of a T2-weighted space 3D sequence. The NCI maps are based on *z* scores using a rescaling factor to visualize subtle differences in a graphically sufficient manner (0-1000). In this case, bilateral rotary saturation effects (in red color) are visible within the thalamus (D, E, F). Note the thickness of the temporal muscles (star) overlying the skull. MRI, magnetic resonance imaging; NCI, neuronal current imaging

TABLE 1 Number of dogs with IE and control dogs showing rotary saturation effects or not

	rotary saturation effect	rotary saturation effect	Total number of patients
Dogs with IE	11	1	12
Control group	1	4	5

Abbreviations: IE, idiopathic epilepsy.

frequency of 120 Hz; in 10 dogs, a positive result was seen at 240 Hz, and in 2 dogs at 480 Hz. In 1 dog with generalized tonic-clonic seizures (dog 6), no abnormal neuronal currents were detected with any of the SL frequencies. In 2 dogs, the rotary saturation effects only appeared in the right hemisphere and in 4 dogs in the left hemisphere whereas 5 dogs had rotary saturation effects in both hemispheres of the forebrain.

In 4 of 5 dogs in the control group, no rotary saturation effects were visible. In 1 dog (dog 14), that was diagnosed with canine neuronal lipofuscinosis by genetic testing (ATP13A2 missense variant) before MRI the pcSIRS yielded a positive result at 240 Hz. After MRI and euthanasia, the diagnosis was confirmed pathologically.[21]

The number of true positive test results was 11 of 12 dogs with epileptic seizures and the number of false positive results was 1 (Table 1). Sensitivity and specificity of pcSIRS to discriminate between dogs with epileptic seizures and control dogs without epilepsy were 91.7% and 80%, respectively.

4 | DISCUSSION

We report the results of an exploratory prospective study to directly visualize neuronal activity in dogs with IE using the spin lock approach in MRI to map neuronal currents related to oscillating magnetic fields in the brain of dogs.

The previously introduced[13] novel pcSIRS sequence to visualize HFOs in human patients with epilepsy showed abnormal neuronal currents in 11 of 12 dogs with IE.

High-frequency oscillations are transient changes in electrical potentials in the EEG in frequency domains above the gamma band (80-600 Hz). Recently, it was discovered that these oscillations have importance as potential markers of epileptogenic areas in the cerebral cortex. The presence of HFOs in epileptic tissue was first detected in rodents with experimentally induced temporal lobe epilepsy after kainic acid injection into the hippocampus[22] and they also have been detected in dogs during experimental conditions.[23] In the presence of HFOs, NCI might offer a method to measure the effects of epilepsy on the magnetic field directly, but few studies have been performed using this method until now. Recently, MR phase shifts at high field MRI (4.7 Tesla) were identified in isolated, intact turtle cerebellum and correlated with the time course of the electrically induced time shifts with local field potentials in the extracted brain tissue.[24] Another study investigated 7 healthy human subjects using a visuomotor activation paradigm employing time-locked magnetic source imaging using a gradient-echo echo-planar image pulse sequence. Using the SL experiment, the investigators identified regional signal decrements caused by local differences in magnetization resulting from the double resonance effect.[25] The method proposed in our study differs from previous studies, because it avoids phase-related effects and enables temporal augmentation of nonhemodynamic resonance effects if a high-frequent magnetic field is present in the epileptic brain.

Fundamental for the design of the proposed technique is the relationship between the observed MR effects and a type of double resonance, an interplay between electromagnetic low frequency pulses from the epileptic brain and the spins prepared by radiofrequency pulses of the scanner transmission hardware. In contrast to other studies,[11,26] our approach employs 2 acquisitions, 1 with SL (SL ON) and 1 without SL (SL OFF) in order to cancel out other effects, such as blood oxygen level-dependent (BOLD) effect, $T1\rho$ and $T2\rho$, B0 inhomogeneities, phase effects, and $T2^*$ effects, by deconvolving SL OFF from SL ON. In this way, the pure rotary saturation effect can be distinguished from arbitrary phase variations, which can be derived from the phase images by calculating the SD along the time dimension. Prominent sources of phase distortions such as strong susceptibility gradients near tissue bone or air boundaries thus are removed. Furthermore, BOLD effects are partially eliminated by a pairwise deconvolution approach of the SL ON/SL OFF measurements. As a mathematical operation, the pairwise deconvolution allows decreasing or canceling the sum of all confounding effects that contribute to the signal differences. Local differences in $T1\rho$ because of pathologic conditions compared to normal brain parenchyma are relatively small (13%),[27] whereas signal differences among brain areas of human patients with epilepsy during spin locking experiments were approximately 5- to 6-fold.[13] Similar differences of effect size were observed in the dogs with epilepsy undergoing the spin-lock experiment. However, we did not implement quantification of the additive effects, but we aim to quantify and correct effects such as B0 inhomogeneities and $T1\rho$ in the future to optimize the method.

For our present study, the sequence was adapted to increase the likelihood of detecting resonant phenomena with neuronal currents. Three spin lock pulses with 120, 240, and 480 Hz were applied accordingly. These frequencies were chosen heuristically, but the values are based on results of EEG in human beings with epilepsy. It remains unclear why the majority of dogs with IE had a positive result to the SL pulse of 240 Hz, whereas none showed saturation effects at 120 Hz in contrast to human beings and only few were detected at 480 Hz. Additional in vivo recordings with simultaneous intracranial EEG recordings would be needed to select the optimal frequency for dogs with epilepsy. Sensitivity to detect resonance phenomena can be improved noninvasively by increasing the number of pulses with different frequencies. However, doing so also increases acquisition time. Future developments therefore will include nonlinear fitting approaches as well as experimental determination of the frequency of the HFOs in the brain before applying SL pulses.

In 1 dog with no history of epileptic seizures, the pcSIRS demonstrated abnormal neuronal currents. This dog was diagnosed by genetic testing with neuronal ceroid lipofuscinosis, and the diagnosis was later confirmed on pathologic examination of the brain.[21] Although the dog did not show apparent seizures, we cannot exclude that the underlying storage disease might have facilitated latent epileptic seizures. We included the results from this dog, because rotary saturation effects were observed, but we cannot determine if they represent false positive effects or subthreshold epileptic activity without overt seizures. Because the pcSIRS technique is designed to detect subtle effects in magnetic fields, it could serve as a screening tool to predict development of epileptic seizures. We therefore included the dog with neuronal ceroid lipofuscinosis in the study population. One false negative result of the pcSIRS occurred in a Havanese-mixed breed dog. This dog had a history of generalized tonic-clonic seizures. The reason for the false negative result in this dog remains unclear, but it is possible that the rather small brain size resulted in difficulty in detecting double resonant saturation from the smaller volume. This argument, however, does not seem to be valid for all small brain volumes, because saturation effects were detected in an even smaller Havanese-mixed breed dog.

Magnetic resonance effects that occurred simultaneously in all 3 frequency bands were observed in all dogs. By mapping the pcSIRS with brain anatomy, these effects could be identified not as epilepsy-associated effects, but effects associated with electromagnetic activity in muscles. This electromagnetic activity within the masticatory muscles overlying the skull in dogs is a major challenge and disadvantage with EEG in veterinary medicine. In contrast to human medicine, the application of scalp EEG is limited by the physiological artifacts caused by muscle contractions and physical artifacts associated with montage of EEG instrumentation or electrodes.[28] Whereas in human patients with epilepsy, systematic investigations that include ictal semiology, EEG, and advanced imaging techniques allow for syndromal classification, the EEG performed before the MRI examination did not identify abnormalities in any dog and prevented such classification.

Performing scalp EEG in dogs under general anesthesia might limit ability to detect abnormal signals.[16] Our study design with EEG performed under general anesthesia therefore was therefore not ideal. Despite its known anticonvulsant properties,[29] propofol does not suppress spontaneous epileptiform activity completely and therefore is considered as an alternative anesthetic agent for dogs undergoing general anesthesia for EEG.[29-31] It seems essential to prevent artifacts generated by contractions of muscles covering the skull.[28,30,32] Therefore, the use of a non-depolarizing peripheral muscle relaxant is reasonable, and its successful application has been described in previous studies.[30] In our study, no abnormalities were detected on EEG recordings, either in dogs classified as having IE or in control dogs. Recent studies showed promising results for scalp EEG in dogs, even with sedation, and EEG abnormalities would be necessary to increase confidence for classification as IE and possibly even to differentiate between focal and generalized epilepsy. For this purpose, longer EEG recordings under sedation are beneficial, but because of limitations of our experimental setting and patient recruitment doing so was not possible in our study. This limitation should be addressed in future studies. Despite the negative result of EEG recording, it was possible to classify dogs into the group of IE according to the criteria proposed by the International Veterinary Epilepsy Task Force (IVETF). Comparing the results of the pcSIRS in this case-control study, a preliminary differentiation between dogs with IE and control dogs was made, but future studies including dogs with structural epilepsy and comparison to the gold standard will be necessary to evaluate the benefit of pcSIRS.

The gold standard to detect HFOs is intracranial EEG. Intracranial EEG recording overcomes the limitations of scalp EEG, but today, the invasiveness, risks, and costs associated with intracranial EEG recording do not justify its applications in dogs with epilepsy.[33,34] A noninvasive additive technique to visualize abnormal neuronal currents in the brain related to IE therefore seems of special relevance for veterinary medicine. Such MRI methods that can support a clinical hypothesis and that can be applied under general anesthesia might allow such a classification if they enable the containment of the potential epileptogenic zone to a hemisphere (following the International League Against Epilepsy concept of focal epilepsy) or on the lobar level (for syndromal classification).[10]

In our study, widespread rotary saturation effects were observed in the brains of dogs with IE. In humans, a combination of imaging and neurophysiological techniques (most frequently structural MRI and EEG) is used to determine the seizure onset zone,[35-40] and previous results in humans showed that neuronal currents detected with the pcSIRS sequence overlap with epileptogenic activity.

So far, it is unknown if the NCI-related saturation effects detected with the pcSIRS sequence are constrained to the epileptogenic zone or rather to the symptomatogenic zone in epileptic networks in dogs. Further application of the method in a larger sample size and its correlation with functional MRI are necessary to allow for further classification of IE in generalized vs focal epilepsy and the identification of a potential epileptogenic zone.

Our study is proof-of-concept that pcSIRS can be applied in dogs and that it detects NCI-related effects in dogs with IE, whereas these effects were absent in all except 1 control dog. The proposed method provides a noninvasive diagnostic tool for veterinary epileptology. It might provide additional knowledge about how to classify dogs with IE by using MRI and offers a new method for imaging research in epilepsy in dogs.

ACKNOWLEDGMENT

No funding was received for this study. The authors thank Osman Limanoski and the team of MR technicians for their generous support.

CONFLICT OF INTEREST DECLARATION

Authors declare no conflict of interest.

OFF-LABEL ANTIMICROBIAL DECLARATION

Authors declare no off-label use of antimicrobials.

INSTITUTIONAL ANIMAL CARE AND USE COMMITTEE (IACUC) OR OTHER APPROVAL DECLARATION

Approved by the Veterinary Office, Canton of Bern, Switzerland—BE15/18 and No. 29935.

HUMAN ETHICS APPROVAL DECLARATION

Authors declare human ethics approval was not needed for this study.

ORCID

Mathieu Raillard https://orcid.org/0000-0003-4057-9312
Daniela Schweizer https://orcid.org/0000-0003-4600-6523

REFERENCES

1. Berendt M, Farquhar RG, Mandigers PJ, et al. International Veterinary Epilepsy Task Force consensus report on epilepsy definition, classification and terminology in companion animals. *BMC Vet Res*. 2015;11:182.
2. Chandler K. Canine epilepsy: what can we learn from human seizure disorders? *Vet J*. 2006;172:207-217.
3. Ghormley TM, Feldman DG, Cook JR Jr. Epilepsy in dogs five years of age and older: 99 cases (2006-2011). *J Am Vet Med Assoc*. 2015;246:447-450.
4. Heske L, Körberg IB, Nødtvedt A, et al. Clinical characteristics of epilepsy of unknown origin in the Rottweiler breed. *Acta Vet Scand*. 2015;57:75.
5. Arrol L, Penderis J, Garosi L, Cripps P, Gutierrez-Quintana R, Gonçalves R. Aetiology and long-term outcome of juvenile epilepsy in 136 dogs. *Vet Rec*. 2012;170:335.
6. Brauer C, Kastner SB, Rohn K, et al. Electroencephalographic recordings in dogs suffering from idiopathic and symptomatic epilepsy: diagnostic value of interictal short time EEG protocols supplemented by two activation techniques. *Vet J*. 2012;193:185-192.
7. James FMK, Cortez MA, Monteith G, et al. Diagnostic utility of wireless video-electroencephalography in unsedated dogs. *J Vet Intern Med*. 2017;31:1469-1476.
8. Utsugi S, Saito M, Sato T, Kunimi M. Relationship between interictal epileptiform discharges under medetomidine sedation and clinical seizures in canine idiopathic epilepsy. *Vet Rec*. 2020;187:67.
9. Wrzosek M, Ives JR, Karczewski M, Dziadkowiak E, Gruszka E. The relationship between epileptiform discharges and background activity in the visual analysis of electroencephalographic examinations in dogs with seizures of different etiologies. *Vet J*. 2017;222:41-51.
10. Scheffer IE, Berkovic S, Capovilla G, et al. ILAE classification of the epilepsies: position paper of the ILAE Commission for Classification and Terminology. *Epilepsia*. 2017;58:512-521.
11. Witzel T, Lin FH, Rosen BR, Wald LL. Stimulus-induced Rotary Saturation (SIRS): a potential method for the detection of neuronal currents with MRI. *Neuroimage*. 2008;42:1357-1365.
12. Abragam A. *Principles of Nuclear Magnetism. International Series of Monographs in Physics*. Vol 32; London: Oxford University Press; 1961.
13. Kiefer C, Abela E, Schindler K, Wiest R. Focal epilepsy: MR imaging of nonhemodynamic field effects by using a phase-cycled stimulus-induced rotary saturation approach with spin-lock preparation. *Radiology*. 2016;280:237-243.
14. Beths T, Glen JB, Reid J, et al. Evaluation and optimisation of a target-controlled infusion system for administering propofol to dogs as part of a total intravenous anaesthetic technique during dental surgery. *Vet Rec*. 2001;148:198-203.
15. Hasegawa D. Diagnostic techniques to detect the epileptogenic zone: pathophysiological and presurgical analysis of epilepsy in dogs and cats. *Vet J*. 2016;215:64-75.
16. Pellegrino FC, Sica REP. Canine electroencephalographic recording technique: findings in normal and epileptic dogs. *Clin Neurophysiol*. 2004;115:477-487.
17. Gallichan D, Marques JP, Gruetter R. Retrospective correction of involuntary microscopic head movement using highly accelerated fat image navigators (3D FatNavs) at 7T. *Magn Reson Med*. 2016;75:1030-1039.
18. Holland D, Kuperman JM, Dale AM. Efficient correction of inhomogeneous static magnetic field-induced distortion in Echo Planar Imaging. *Neuroimage*. 2010;50:175-183.
19. Kuwabara T, Hasegawa D, Kobayashi M, et al. Clinical magnetic resonance volumetry of the hippocampus in 58 epileptic dogs. *Vet Radiol Ultrasound*. 2010;51:485-490.
20. Pruessner JC, Li LM, Serles W, et al. Volumetry of hippocampus and amygdala with high-resolution MRI and three-dimensional analysis software: minimizing the discrepancies between laboratories. *Cereb Cortex*. 2000;10:433-442.
21. Schmutz I, Jagannathan V, Bartenschlager F, et al. ATP13A2 missense variant in Australian Cattle Dogs with late onset neuronal ceroid lipofuscinosis. *Mol Genet Metab*. 2019;127:95-106.
22. Bragin A, Engel J Jr, Wilson CL, et al. Electrophysiologic analysis of a chronic seizure model after unilateral hippocampal KA injection. *Epilepsia*. 1999;40:1210-1221.
23. Cimbálník J, Hewitt A, Worrell G, Stead N. The CS algorithm: a novel method for high frequency oscillation detection in EEG. *J Neurosci Methods*. 2018;293:6-16.
24. Sundaram P, Nummenmaa A, Wells W, et al. Direct neural current imaging in an intact cerebellum with magnetic resonance imaging. *Neuroimage*. 2016;132:477-490.
25. Xiong J, Fox PT, Gao JH. Directly mapping magnetic field effects of neuronal activity by magnetic resonance imaging. *Hum Brain Mapp*. 2003;20:41-49.
26. Redfield AG. Nuclear magnetic resonance saturation and rotary saturation in solids. *Phys Rev*. 1955;98:22.
27. Haris M, McArdle E, Fenty M, et al. Early marker for Alzheimer's disease: hippocampus T1rho (T(1rho)) estimation. *J Magn Reson Imaging*. 2009;29:1008-1012.
28. De Risio L, Bhatti S, Muñana K, et al. International Veterinary Epilepsy Task Force consensus proposal: diagnostic approach to epilepsy in dogs. *BMC Vet Res*. 2015;11:148.
29. Bergamasco L, Accatino A, Priano L, Neiger-Aeschbacher G, Cizinauskas S, Jaggy A. Quantitative electroencephalographic findings in beagles anaesthetized with propofol. *Vet J*. 2003;166:58-66.
30. Brauer C, Kastner SB, Schenk HC, et al. Electroencephalographic recordings in dogs: prevention of muscle artifacts and evaluation of two activation techniques in healthy individuals. *Res Vet Sci*. 2011;90:306-311.
31. Jaggy A, Bernardini M. Idiopathic epilepsy in 125 dogs: a long-term study. Clinical and electroencephalographic findings. *J Small Anim Pract*. 1998;39:23-29.
32. Cauduro A, Dondi M, Favole P, Opreni M, Simonetto LA, Lorenzo V. Artifacts during short-term interictal electroencephalographic recording in dogs. *J Am Anim Hosp Assoc*. 2017;53:80-89.
33. Davis KA, Sturges BK, Vite CH, et al. A novel implanted device to wirelessly record and analyze continuous intracranial canine EEG. *Epilepsy Res*. 2011;96:116-122.
34. Davis KA, Ung H, Wulsin D, et al. Mining continuous intracranial EEG in focal canine epilepsy: relating interictal bursts to seizure onsets. *Epilepsia*. 2016;57:89-98.
35. Bouet R, Mauguière F, Daligault S, et al. The relationship between morphological lesion, magnetic source imaging, and intracranial stereo-electroencephalography in focal cortical dysplasia. *Neuroimage Clin*. 2017;15:71-79.
36. Centeno M, Tierney TM, Perani S, et al. Combined electroencephalography-functional magnetic resonance imaging and

electrical source imaging improves localization of pediatric focal epilepsy. *Ann Neurol*. 2017;82:278-287.
37. Chen Z, An Y, Zhao B, et al. The value of resting-state functional magnetic resonance imaging for detecting epileptogenic zones in patients with focal epilepsy. *PLoS One*. 2017;12:e0172094.
38. Khoo HM, Hao Y, von Ellenrieder N, et al. The hemodynamic response to interictal epileptic discharges localizes the seizure-onset zone. *Epilepsia*. 2017;58:811-823.
39. Luders HO, Najm I, Nair D, et al. The epileptogenic zone: general principles. *Epileptic Disord*. 2006;8(suppl 2):S1-S9.
40. Nedic S, Stufflebeam SM, Rondinoni C, et al. Using network dynamic fMRI for detection of epileptogenic foci. *BMC Neurol*. 2015;15:262.

SUPPORTING INFORMATION

Additional supporting information may be found in the online version of the article at the publisher's website.

How to cite this article: Unger DM, Wiest R, Kiefer C, et al. Neuronal current imaging: An experimental method to investigate electrical currents in dogs with idiopathic epilepsy. *J Vet Intern Med*. 2021;1-9. doi:10.1111/jvim.16270